



Characterization of Precipitates in Mechanically Alloyed SUS304L Type Steel with Zirconium Addition

Daniel Morrall^{1,2*}, Jin Gao², Zhexian Zhang², Kiyohiro Yabuuchi², Akihiko Kimura², Takahiro Ishizaki³ and Yusaku Maruno³

¹Graduate School of Energy Science, Kyoto University, Japan

²Institute of Advanced Energy, Kyoto University, Japan

³Research & Development Group, Hitachi Ltd., Japan

Abstract

A mechanically alloyed austenitic stainless steel (MA304LZ) was produced from pre-alloyed SUS304L powder with 0.7% wt of Zr addition. The precipitates had a bimodal size distribution causing strengthening of MA304LZ with 3.3 times larger yield stress than SUS304L, although the contribution of fine grains of MA304LZ to the strengthening was larger than the dispersion of precipitates. For precipitate characterization, two types of extraction replica samples were produced; 1) Thin carbon film and 2) Electrochemically dissolved residue. Extraction replica residue was analyzed using XRD and both types were attached to copper grids for TEM, EDS, and EELS analysis. The previously reported Zr-rich precipitates were revealed to be ZrO₂ (zirconia) with no evidence of ZrN or ZrC.

Keywords

TEM, XRD, Zirconia, Precipitation hardening

Introduction

Enhancing the safe operation of nuclear reactors is of upmost importance for meeting future energy demands [1]. Currently zircaloy is used as a fuel cladding material which has many desirable characteristics under moderate conditions. However, in extreme conditions hydrogen generation can become extremely problematic and as such research into alternative cladding materials has received greater interest [2]. Iron-based stainless steels have been proposed as one alternative material due to having several desirable characteristics: 1) High corrosion resistance even in extreme conditions, 2) Chemically stable at high temperatures, 3) No α' embrittlement that can plague ferritic/martensitic (F/M) steels under radiation [3]. Austenitic stainless steels carry with them their own set of issues, chiefly the well-known issue of void swelling at relatively low dpa [4-6].

Creating an ideal material for use in nuclear applications would need to have sufficiently high strength at high temperatures, high corrosion resistance, and a high degree of radiation tolerance. Currently much research has been completed on F/M steels with the addition of nano-sized oxides which have been shown to improve several characteristics of the F/M steels such as radiation tolerances and yield strength through several mechanisms [7-9]. Especially, Kimura, et al. developed 15Cr-5Al-ODS ferritic steels added with small amount of Zr [10-14] which showed a significant strengthening of Al-added ODS steels, which was due to the alternation of the lower number density of coarse (Y, Al) oxides with higher number density of fine (Y, Zr) oxides [10,15,16].

Subsequently, the addition of nano-sized oxide particles can be used to improve the void swelling issue and relatively lower strength of austenitic stainless steel in

***Corresponding author:** Daniel Morrall, Graduate School of Energy Science, Kyoto University, Yoshida-honmachi, Sakyou-ku, Kyoto, 606-8501, Japan; Institute of Advanced Energy, Kyoto University, Gokasho, Uji, Kyoto 611-0011, Japan, Tel: +81-774-38-3478, E-mail: moraru.danieru.43v@st.kyoto-u.ac.jp

Received: June 09, 2018; Accepted: July 09, 2018; Published: July 11, 2018

Copyright: © 2018 Morrall D, et al. This is an open-access article distributed under the terms of the Creative Commons Attribution License, which permits unrestricted use, distribution, and reproduction in any medium, provided the original author and source are credited.

Citation: Morrall D, Gao J, Zhang Z, Yabuuchi K, Kimura A, et al. (2018) Characterization of Precipitates in Mechanically Alloyed SUS304L Type Steel with Zirconium Addition. Int J Metall Met Phys 3:015

Table 1: Chemical Compositions of MA304LZ.

wt. %	C	Si	Mn	P	S	Cr	Ni	Zr	O	N	Fe
MA304LZ	0.02	Si	0.15	0.018	0.001	19.5	11.18	0.7	0.018	0.074	Bal

order to take advantage of the high corrosion resistance and favorable high temperature stability. These oxide dispersion strengthened (ODS) austenitic steels will be greatly dependent on the structural and chemical nature of the oxide particles formed [3].

In our previous work, we reported the high yield strength of 767 MPa in a mechanically alloyed austenitic stainless steel with Zr addition (MA304LZ) accompanied by the presence of nano-sized precipitate formation and its effects on the microstructure [17], the yield strength of 304L SS was around 230 MPa. Although precipitates were observed in the previous study, the exact chemical compositions remained unclear. The formation of ZrN, ZrC, or ZrO₂, were the most likely candidates and each have unique properties which can affect the overall material differently [18-22]. In this study we present the results of in-depth chemical analyses of the precipitates which may contribute to the strengthening of MA304LZ steel.

Experimental

The analyzed austenitic stainless steel (MA304LZ) was produced from pre-alloyed SUS304L powder and high purity (99.9%) Zr powder (suspended in water) at 0.7 wt.%. The mixed powder was obtained by milling in a P-5 Fritsch planetary ball mill at 200 rpm for 48 hours in an argon environment with a ball-to-powder ratio of 9:10 in weight. Both the milling balls and milling chamber were composed of SUS304 stainless steel. A rather low ball-to-powder ratio along with low rotation speed was used to alleviate the affixing issue of the resulting powder to the mixing pot which has been encountered by previous researchers [3,23]. The milled powder was encapsulated in a steel tube and evacuated in a vacuum of 1×10^{-3} Pa for degassing. Then consolidated through hot isostatic pressing (HIP) at 140 MPa after heating to 950 °C at a heating rate of 300 °C/h. The consolidated bulk material was annealed in Ar gas at 1000 °C for 30 min followed by quenching into water at ambient temperature. The chemical composition of the steel is shown in Table 1.

Two types of specimens were prepared for TEM observation, extraction replica and bulk electrochemically thinned samples. TEM bulk specimens were prepared with a Struers twinjet electropolisher at 18 V in a 90% CH₃OH 10% HClO₄ electrolyte at -20 °C. Extraction replica samples were produced by applying a thin layer of carbon to the surface of MA304LZ after etching with aqua regia (HNO₃ + HCl) followed by electrochemical dissolving the matrix and attaching the carbon ex-

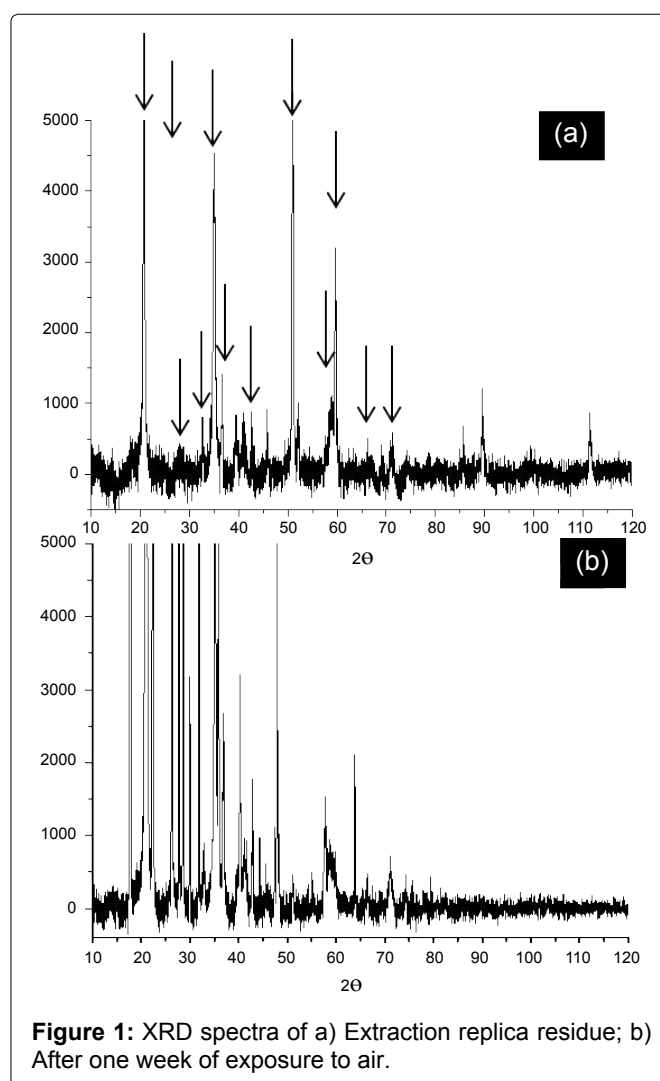


Figure 1: XRD spectra of a) Extraction replica residue; b) After one week of exposure to air.

traction replica layer to a copper mesh. TEM, EDS, and EELS observations were conducted using a JEM 2200FS Schottky emission FE-TEM with an accelerating voltage of 200 kV.

X-ray diffraction spectroscopy (XRD) was carried out on bulk and extraction replica residue of MA304LZ. Extraction replica residue specimens were prepared by electrochemically dissolving a bulk piece of MA304LZ in 10% HCl 90% CH₃OH followed by vacuum filtering the solution. XRD measurements were taken using a Rigaku RINT-TTRIII/KE XRD in the range of $2\theta = 10^\circ$ - 120° with a Co-K α filament at 250 mA and 40 kV.

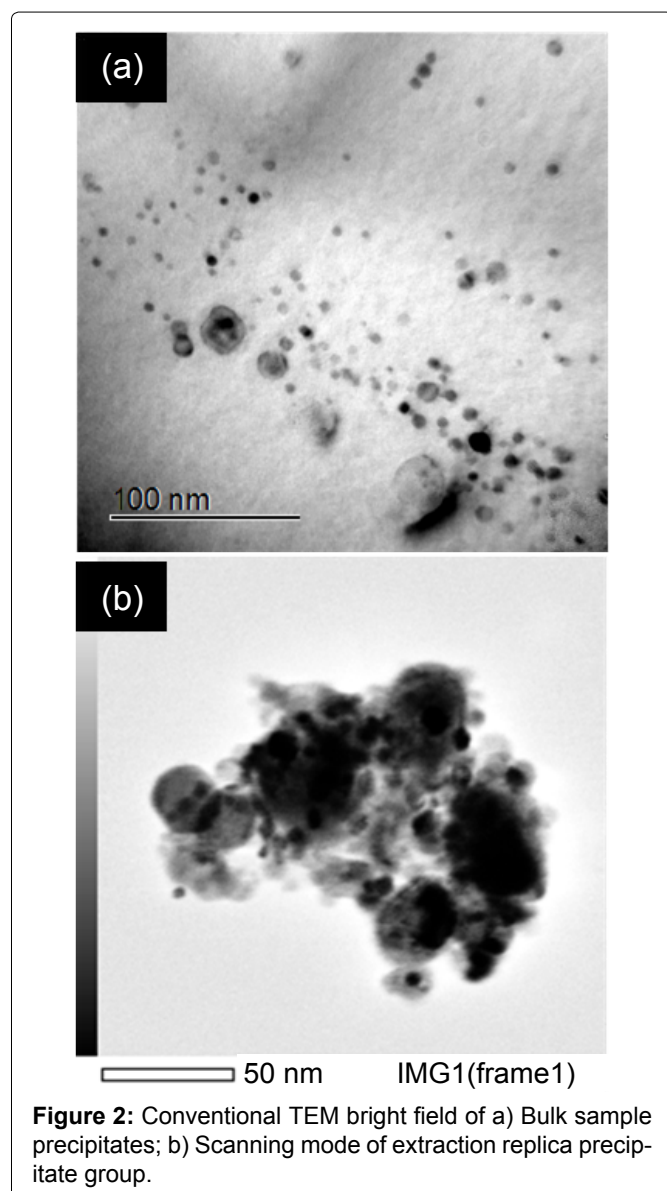
Results and Discussion

Crystalline structure

XRD patterns of extraction replica residues are shown in Figure 1. Figure 1b is the same residue as that of Figure 1a but after allowing the sample to sit in air for one

Table 2: Averaged values of XRD reflection locations appearing more than once (a) Un-aged extraction residue, (b) After 1-week exposure to air.

(a) Consistent	20.78	27.93	32.34	34.91	36.64	42.56	51.03	57.72	59.53	66.22	70.97	
(b) Retained after aging	20.75	27.95	36.68	40.21	42.73	45.63	51.09	57.74	59.22	66.42	70.88	74.3



week for observing the changes induced by atmospheric effects. The residues were each prepared using the same methods and conditions however there are some differences between these patterns. Electrochemically dissolving bulk MA304LZ followed by vacuum filtering seems to produce varying results making replication difficult, however there were some commonly observed values of 2θ which are denoted in Figure 1a with arrows and listed in Table 2. The atmospherically contaminated sample showed very significant differences from a week of exposure to air, most notably is the appearance of several reflections below 35° and the disappearance of all the reflections above 80° . The XRD pattern of bulk MA304LZ was previously reported in [17] with only a few reflections that were consistent with an γ -phase structure while

containing a small amount of α' -phase (110), which is considered to be deformation induced martensite in unstable 304L type austenitic stainless steel.

The consistently observed reflections at or near $2\theta = 36.7, 42.6, 74.3$ suggest the presence of FCC phase ZrO_2 [24]. After aging in air for one week these reflection locations remained, however the new reflections at $2\theta = 40.3, 41.2, 59.71, 63.8$ are consistent with tetragonal ZrO_2 suggesting that exposure to air allows for the formation of tetragonal crystalline structure of ZrO_2 [25]. However, the inconsistent XRD spectra across samples make it difficult to exclude the possibility of carbide or nitride formation.

Chemical compositions

Conventional TEM and STEM images of bulk and extraction replica samples are shown in Figure 2a and Figure 2b, respectively. In our previous work, observed precipitates were found to have a large variation in size and number density particularly in the homogeneity of distribution (larger precipitates were found to have a more homogeneous distribution while smaller precipitates had a rather inhomogeneous distribution) [17]. The particle size in the extraction residue for XRD measurement matches those observed by STEM.

Energy dispersive spectra (EDS) of bulk samples are shown in Figure 3 and confirmed that the precipitates were Zr-rich however matrix interference made it impossible to confirm or exclude the existence of oxides, carbide, or nitrides. EDS observations of over 30 precipitates and precipitate clusters were conducted, a representative precipitate found in the extraction replica samples is shown in Figure 4. All the analyzed precipitates demonstrated a high concentration of both Zr and O in ratios that correlate with ZrO_2 , however, no nitrides or carbides were observed. Additionally, a tendency for the precipitates to conglomerate together was also observed in several extraction replica samples. The electron energy loss spectrum (EELS) of several precipitates in a bulk sample was conducted to determine the presence of nitrogen and is shown in Figure 5. An EELS peak at 401 eV is expected for nitrogen, however no such peak was observable.

Oxide particle dispersion is well known as a strengthening mechanism of metallic materials, where the nano-sized particles in high number density are obstacles for dislocation motion, and inter-particle distance is critical to determine strengthening [10-14]. In the present material (MA304LZ) an addition of a small amount of

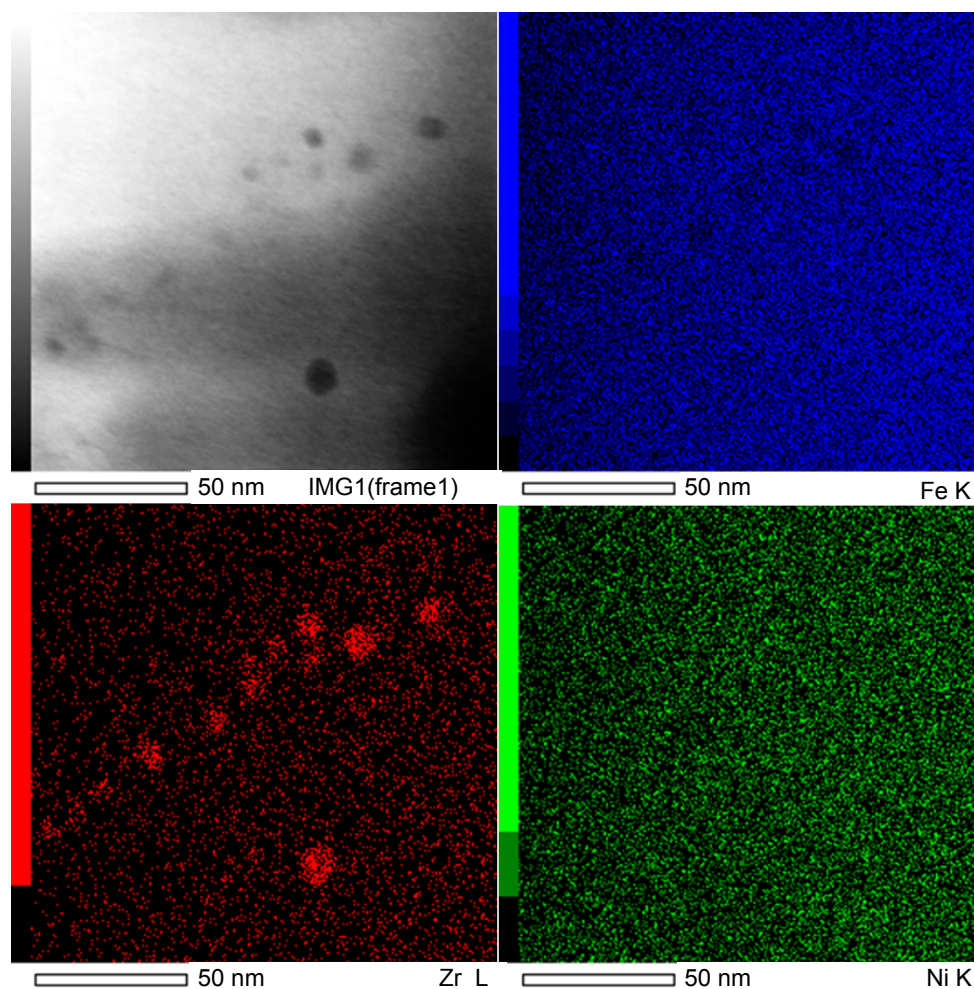


Figure 3: EDS map of precipitates in a bulk sample.

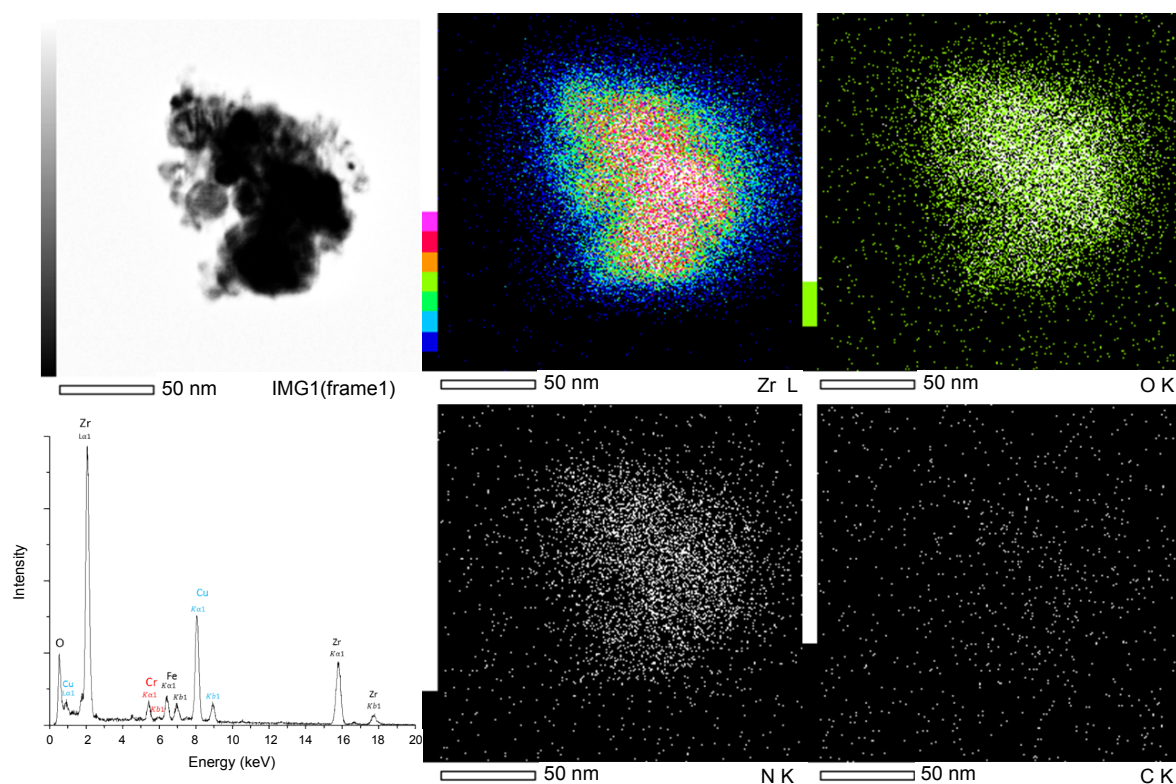


Figure 4: EDS spectra and mapping of extraction replica precipitate group.

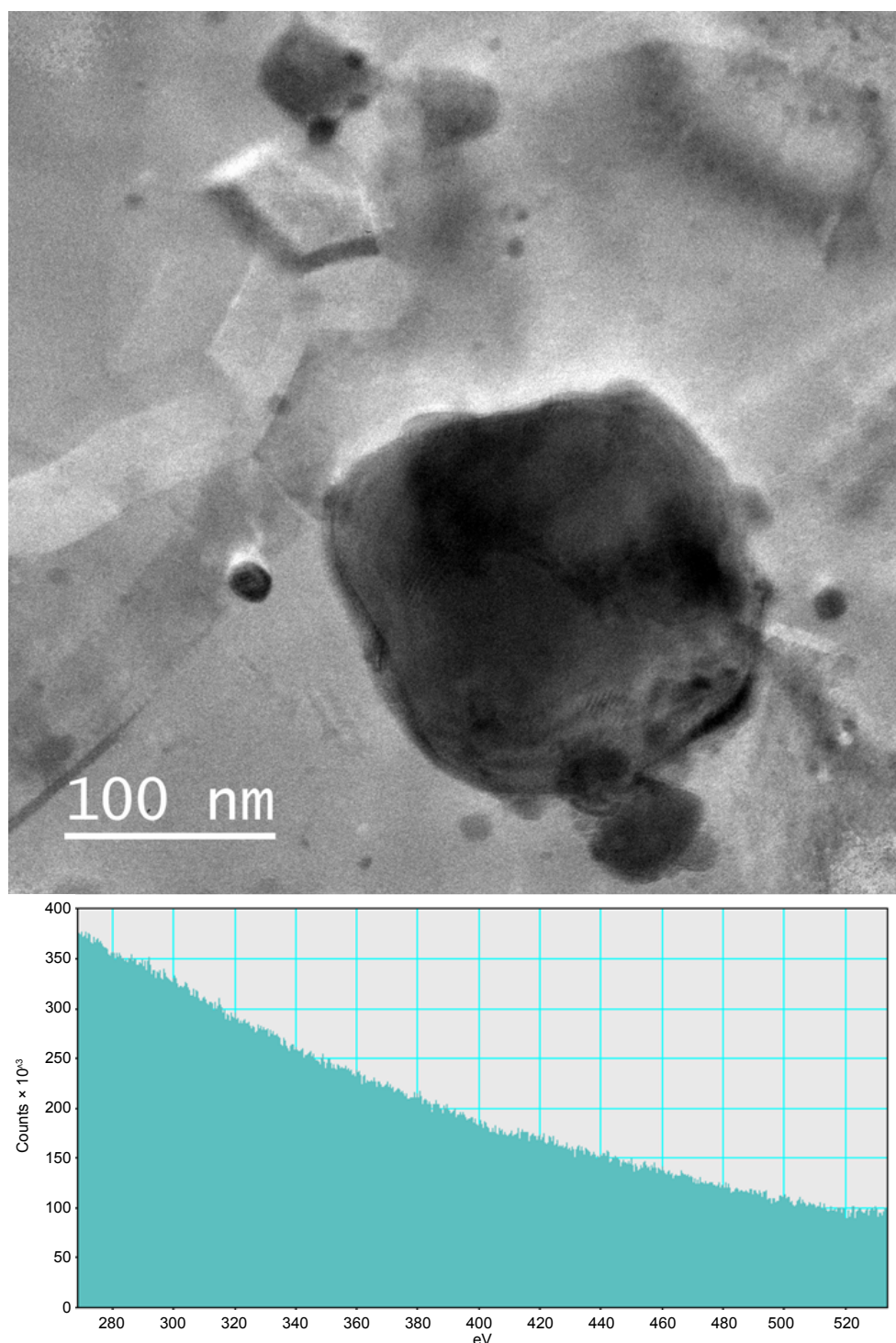


Figure 5: EELS of precipitates in a bulk sample.

Zr resulted in the formation of ZrO_2 of which the averaged diameter was 6.0 nm [17]. Although the oxides are more stable than nitrides and carbides based on thermodynamics, the largest concern was the contamination of nitrogen from air during exposure of mixed powder to air and carbon from the Cr-C steel balls during mechanical alloying. This contamination may cause consumption of Zr and reduce the total amount of fine ZrO_2 , and consequently reducing the yield strength of MA304LZ steel. However, it can be concluded that no remarkable

formation of nitride nor carbide was observed in this study, which resulted in maintaining the strengthening of Zr-added MA304L austenitic stainless steel.

Conclusions

A mechanically alloyed austenitic stainless steel (MA304LZ) was produced from pre-alloyed SUS304L powder added with 0.7% wt. of Zr. The combined observations of XRD, TEM, EDS, and EELS lead to several conclusions about precipitation behavior in MA304LZ.

1. XRD observations indicate the presence of ZrO_2 with an FCC structure, however the existence of ZrN or ZrC could not be excluded due to a lack of consistency in XRD patterns.
2. TEM and EDS observations indicated the chemical composition of the nanosized precipitates to be ZrO_2 , no ZrN or ZrC were observed in over 30 precipitate groups.
3. EELS observations clearly demonstrated a lack of nitrides or carbide. The addition of high-purity Zr to pre-alloyed 304 steel powder in a ball mill seems to either exclusively or predominately produce thermodynamically favorable ZrO_2 oxides.

Acknowledgements

The authors would like to express gratitude to the Japanese Ministry of Education, Culture, Sports, Science and Technology (MEXT) for their financial support. Also, gratitude is extended towards the Hitachi Corporation for contribution of the MA304LZ material for study.

References

1. SJ Zinkle, GS Was (2013) Materials challenges in nuclear energy. *Acta Materialia* 61: 735-758.
2. CM Silva, KJ Leonard, E Van Abel, JW Geringer, CD Bryan (2018) Investigation of mechanical and microstructural properties of Zircaloy-4 under different experimental conditions. *Journal of Nuclear Materials* 499: 546-557.
3. Y Miao, K Mo, Z Zhou, X Liu, K Lan, et al. (2016) Size-dependent characteristics of ultra-fine oxygen-enriched nanoparticles in austenitic steels. *Journal Nuclear Materials* 480: 195-201.
4. C Sun, FA Garner, L Shao, X Zhang, SA Maloy (2017) Influence of injected interstitials on the void swelling in two structural variants of 304L stainless steel induced by self-ion irradiation at 500 °C. *Nuclear Instruments and Methods in Physics Research Section B: Beam Interactions with Materials and Atoms* 409: 323-327.
5. PL Maziasz, JT Busby (2012) Properties of austenitic steels for nuclear reactors applications. *Comprehensive Nuclear Materials* 2: 267-283.
6. H Jin, E Ko, S Lim, J Kwon, C Shin (2017) Effect of irradiation temperature on microstructural changes in self-ion irradiation austenitic stainless steel. *Journal of Nuclear Materials* 493: 239-245.
7. K Mo, Z Zhou, Y Miao, D Yun, H Tung (2014) Synchrotron study on load partitioning between ferrite/martensite and nanoparticles of a 9Cr ODS Steel. *Journal of Nuclear Materials* 455: 376-381.
8. DT Hoelzer, J Bentley, MA Sokolov, MK Miller, GR Odette (2007) Influence of particle dispersions on the high-temperature strength of ferritic alloys. *Journal of Nuclear Materials* 367: 166-172.
9. RL Klueh, DS Gelles, S Jitsukawa, A Kimura, GR Odette (2002) Ferritic/martensitic steels-overview of recent results. *Journal of Nuclear Materials* 307-311: 455-465.
10. A Kimura, R Kasada, N Iwata, H Kishimoto, CH Zhang, et al. (2011) Development of Al added high-Cr ODS steels for fuel cladding of next generation nuclear systems. *Journal of Nuclear Material* 417: 176-179.
11. A Kimura, S Ukai, M Fujiwara (2003) Development of fuel clad materials for high burn-up operation of LWR. *International Conference on Global Environment and Advanced Nuclear Power Plants*, Kyoto Research Park, 15-19.
12. JS Lee, A Kimura, S Ukai, M Fujiwara (2004) Effects of hydrogen on the mechanical properties of oxide dispersion strengthening steels. *Journal of Nuclear Material* 329-333: 1122-1126.
13. K Yutani, R Kasada, H Kishimoto, A Kimura (2007) Irradiation hardening and microstructure evolution of ion-irradiated ods ferritic steels. *Journal of ASTM International* 4: 100701.
14. J Isselin, R Kasada, A Kimura, T Okuda, M Inoue (2010) Effects of Zr addition on the microstructure of 14%Cr4%Al ODS ferritic steels. *Materials Transactions* 51: 1011-1015.
15. P Dou, A Kimura, T Okuda, M Inoue, S Ukai (2011) Polymorphic and coherency transition of Y-Al complex oxide particles with extrusion temperature in an Al-alloyed high-Cr oxide dispersion strengthened ferritic steel. *Acta Materialia* 59: 992-1002.
16. P Dou, A Kimura, R Kasada, T Okuda, M Inoue (2014) TEM and HRTEM study of oxide particles in an Al-alloyed high-Cr oxide dispersion strengthened steel with Zr addition. *Journal of Nuclear Material* 444: 441-453.
17. D Morrall, J Gao, Z Zhang, K Yabuuchi, A Kimura, et al. (2018) Tensile properties of mechanically alloyed Zr added austenitic stainless steel. *Nuclear Materials and Energy* 15: 92-96.
18. X Ren, Z Peng, C Wang, Z Fu, L Qi, et al. (2015) Effect of ZrC nano-powder addition on the microstructure and mechanical properties of binderless tungsten carbide fabricated by spark plasma sintering. *International Journal of Refractory Metals and Hard Materials* 48: 398-407.
19. XJ Zhao, DL Chen, HQ Ru, N Zhang (2011) Zirconium nitride nano-particulate reinforced Alon composites: Fabrication, mechanical properties and toughening mechanisms. *Journal of the European Ceramic Society* 31: 883-892.
20. C Gagliardi, RT Alarcon, R De Godoi Machado, DSS Pado-vini, FML Pontes (2017) Thermal study of ZrO_2 nanoparticles: Effect of heating and cooling cycles on the solid-solid transition. *Thermochimica Acta* 653: 59-61.
21. O Malek, B Lauwers, Y Perez, P De Baets, J Vleugels (2009) Processing of ultrafine ZrO_2 toughened WC composites. *Journal of the European Ceramic Society* 29: 3371-3378.
22. P Kempter, RJ Fries (1960) Crystallographic Data. 189. Zirconium Carbide. *Analytical Chemistry* 32: 570.
23. T Gräning, M Rieth, J Hoffmann, A Möslang (2017) Production, microstructure and mechanical properties of two different austenitic ODS steels. *Journal of Nuclear Materials* 487: 348-361.
24. P Bouvier, E Djurado, G Lucazeau, T Le Bihan (2000) High-Pressure structural evolution of undoped tetragonal nanocrystalline zirconia. *Physical Review B* 62: 8731-8737.
25. E Djurado, P Bouvier, G Lucazeau (2000) Crystallite size effect on the tetragonal-monoclinic transition of undoped nanocrystalline zirconia studied by XRD and Raman spectroscopy. *Journal of Solid State Chemistry* 149: 399-407.